Attosecond time delay and confinement resonances in photoionization of endohedral atoms: Xe@C$_{60}$

P. C. Deshmukh, A. Mandal and S. Saha

Department of Physics, Indian Institute of Technology Madras, Chennai-600036, India and
Department of Physics, CPGS, Jain University, Bangalore, 560011, India

A. S. Kheifets

Research School of Physics and Engineering, The Australian National University, Canberra ACT 0200, Australia

V. K. Dolmatov

Department of Physics and Earth Science, University of North Alabama, Florence, AL 35632, USA

S T Manson

Department of Physics and Astronomy, Georgia State University, Atlanta, GA 30303, USA
(Dated: February 4, 2014)

We make a theoretical prediction and study numerically confinement resonances in photoelectron group delay (Wigner time delay) following ionization of an atom encapsulated inside the hollow cage of C$_{60}$. Even though these resonances present the most direct manifestation of the Wigner time delay theory, they have been missed in a previous theoretical investigation of Ar@C$_{60}$ [PRL **111**, 203003 (2013)]. We demonstrate the clear presence of these resonances in time delay of the $4d$ shell of Xe@C$_{60}$.

Unprecedented advances in experimental techniques in measuring time intervals at the attosecond level [1] have engendered the ability to scrutinize the time delay in photoionization of atomic systems in the laboratory [2–4], thereby allowing us to probe the fundamental process of photoionization in the time domain. Specifically, using attosecond pulses of electromagnetic radiation, the time difference between the emergence of photoelectrons from two neighboring atomic subshells has been measured both in Ne [3] and Ar [4, 5]. These experimental results have stimulated a host of theoretical calculations to explain and to further explore this phenomenon [6–9]. This is of great interest, not only as a new way to study a fundamental process of nature, but also as an outstanding, unique opportunity towards an advanced knowledge of the most informative parameter of the process, the photoionization matrix element. This is because the time delay is related to the energy derivative of the phase of the matrix element driving the process [10]. Indeed, the only exploited to date way for getting most of experimental information on photoionization lies through the set of measurements of total and differential photoionization cross sections, but allows only the absolute values and relative phases of matrix elements to be deduced. This way is known as a "complete photoionization experiment" [11]. Time delay investigations, however, go beyond the "complete experiment" strategy and yield the derivative of the phase with respect to the photoelectron energy. Time delay investigations, thus, provide a new avenue to discern the characteristics of the basic physical quantity - the matrix element - and, thus, of the photoionization phenomenon by itself. It is the ultimate aim of this paper to expand time delay studies towards situations where they have never been explored yet.

The theory of time delay in physics was developed some time ago [12] and was originally envisioned as a way to study resonances - the temporary trapping of one (or more) electrons in a quasi-bound state or a potential well. Indeed, the Breit-Wigner formula of resonant scattering $\tau = 2/\Gamma$ equates the time delay τ with the resonant width Γ at half maximum of the cross-section [13]. Resonances are ubiquitous in photoionization of atoms, and these resonances can be of different nature: inner-shell excitations, two-electron excitations, shape resonances, etc. Of recent drastic interest to investigators, which has shaped an area of extremely active modern research activities [14], have become studies of the resonances, termed confinement resonances. The latter occur in the photoionization of an atom A trapped at the center of a C$_{60}$ molecule, the $A@C_{60}$ endohedral atom. The phenomenon of confinement resonances was predicted theoretically long ago (see, e.g., [15]). However, it is only fairly recently that confinement resonances have been studied in depth in numerous theoretical studies at various levels of sophistication [16–19] and references therein], and only very recently verified experimentally in the photoionization of endohedral atoms [20]. Confinement resonances have been explained as interferences between the photoelectron wave emitted directly, and those that experience one or more scattering off the walls of the encapsulating fullerene [21].

If this explanation is correct, these multiple scatterings should show up in the time delay of the photoelectron relative to the time delay of the free atom. It is, however, not at all clear beforehand as to what degree time delay of atomic photoionization can be modified by

confining an atom inside of C_{60} compared to the free atom. Moreover, a recent theoretical study of time delay in Ar@C_{60} [22] have not revealed any confinement resonances in the time delay at all. At the same time, confinement resonances were clearly seen in time delay of of a model system He$^+$@C_{60} [23]. This system, however, was unstable and the theoretical analysis was performed on a one-electron level. Therefore we are presented with the task of unraveling the confinement resonances in a realistic atomic system with the full account of electron correlation.

In this Letter, we explore photoionization of the $4d$ subshell of Xe@C_{60} , where confinement resonances have been found experimentally [20]. Specifically, we focus upon how the time delay can be used to characterize the confinement resonances, along with the time delay phenomenology produced by the resonances. A model potential is employed to introduce the effects of the confining C_{60} on the encaged Xe atom. This should be adequate because the $4d$ subshell is so deeply bound that it cannot hybridize with any of the levels of C_{60} , and the photon energy range (80 to 160 eV) is well away from the C_{60} plasmons so that interchannel coupling with atomic photoionization is not important. Furthermore, recent calculations employing such a model resulted in rather good agreement with the experimental confinement resonances [24]. To properly account for correlations, the calculations are performed within the framework of the random-phase approximation, both the nonrelativistic [25] and relativistic [26] versions; this has the advantages of having a check on each of the calculations, along with giving us the ability to spotlight any relativistic effects.

The time delay is calculated from the photoionization amplitude as $\tau = d\arg f(E)/dE \equiv \mathrm{Im}\left[f'(E)/f(E)\right]$. The amplitude $f(E)$ is given by the partial wave expansion

$$f(E) \propto \sum_{l=l_i\pm 1} e^{i\delta_l} i^{-l} Y_{lm}(\hat{k}) (-1)^m \begin{pmatrix} l & 1 & l_i \\ -m & 0 & m_i \end{pmatrix} \times \langle El\|D\|n_i l_i\rangle \qquad (1)$$

evaluated in the $\hat{z}$ direction of the polarization axis of light. In the RPA method, the reduced dipole matrix element $\langle El\|D\|n_i l_i\rangle$ is evaluated by solving a set of integro-differential equations exhibited graphically by diagrams of Fig. 1. In the absence of inter-shell correlation, the dipole matrix element is represented by the left-most diagram which corresponds to the photon absorption and electron emission from the same shell. The inter-shell correlation allows for the photon absorption by the shell $n_j l_j$ and the electron emission from the shell $n_i l_i$. This process is shown by the two remaining diagrams in which the inter-shell correlation precedes or follows the photon absorption (time-reverse and time-forward diagrams, respectively). The exchange leads to the two ladder-type diagrams (not shown) in addition to the two bubble-type diagrams shown in Fig. 1.

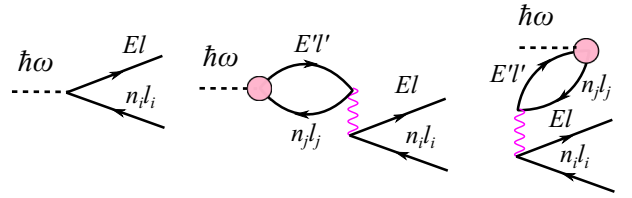The same matrix element is used to evaluate the partial

FIG. 1: (Color online) Graphical representation of the RPA equations. Left: non-correlated dipole matrix element. Center: time-forward process. Right: time-reverse process.

photoionization cross-section from an occupied state $n_i l_i$ to the photoelectron continuum state El

$$\sigma_{n_i l_i \to El}(\omega) = \frac{4}{3}\pi^2 \alpha a_0^2 \omega \left| \langle El\|D\|n_i l_i\rangle \right|^2 \ . \qquad (2)$$

Here α is the fine structure constant and a_0 is the Bohr radius. The occupied orbitals $n_i l_i$ and continuous orbitals El are obtained by the self-consistent field [27] and frozen-core field [28] Hartree-Fock methods. For the present case of the $4d$ shell in Xe, correlations with the $5s$ and $5p$ shells are included resulting in 5 non-relativistic channels. The fullerene shell is modeled by a central potential with the following parameters: the inner shell radius $R_{\mathrm{inner}} = 5.8$ a.u., the width $\Delta = 1.9$ a.u and the depth $U_0 = 0.302$ au.

In the RRPA method, a truncated version was employed to get the photoionization parameters. RRPA accounts for correlations in the initial states and also in the final states by accounting for all the ring-diagrams. The truncated version permits the selection of the interchannel coupling in the final states, restricting the calculation to a sufficient set of photoionization channels that are of importance. The loss of gauge invariance due to truncation, between the length and the velocity forms of the photoionization cross-section, is nominal. In the present RRPA calculation, final state correlations are included through interchannel coupling between all the 13 relativistic dipole channels originating in the $5p$, $5s$ and $4d$ subshells which are open for photoionization in the energy range studied in the present work.

The main results of our work are shown in Fig. 2. On the top set of panels, we display the $4d$ partial photoionization cross-sections for the free (left) and confined (right) Xe atoms. The RRPA results are shown for the spin-resolved $4d_{1/2}$ and $4d_{3/2}$ subshells leading to the ϵf ionization continuum. The cross-sections are weighted with the inverse statistical factors (5/2 and 5/3) to facilitate the shape comparison. The RPA results are shown for the $4d \to \epsilon f$ and $4d \to \epsilon p$ transitions, the former is clearly dominant away from its Cooper minimum. This allows us to concentrate on the cross-section and time delay analysis in the dominant channel only. The RPA and RRPA cross-section results are very close for the free Xe atom after a small photon energy adjustment is made to accommodate different $4d$ ionization thresholds in RRPA (theoretical) and RPA (experimen-

tal). The cross-sections for Xe@C$_{60}$ are qualitatively similar between the two methods, although the RPA predicts sharper resonances at lower photon energy end.

On the bottom set of panels, we show the Wigner time delay results for the free (left) and confined (right) Xe atoms. Agreement of the two methods for the free Xe atom are good except for lower photon energy end where one sees a strong deviation between the spin-resolved $4d$ states. The RPA delay is close to the RRPA $4d_{3/2} \rightarrow \epsilon f_{5/2}$ delay. For Xe@C$_{60}$, the two methods shows the

same set of confinement resonances. The precise shape of the lowest resonance is somewhat dependent of the spin-orbit splitting (see more in [29]). We note that the confinement resonances are much more prominent in the time delay than in the cross-section. The peak of the cross-section corresponds to a dip of the time delay. This is so because the time delay is inversely proportional to the amplitude while the cross-section is quadratic with the amplitude.
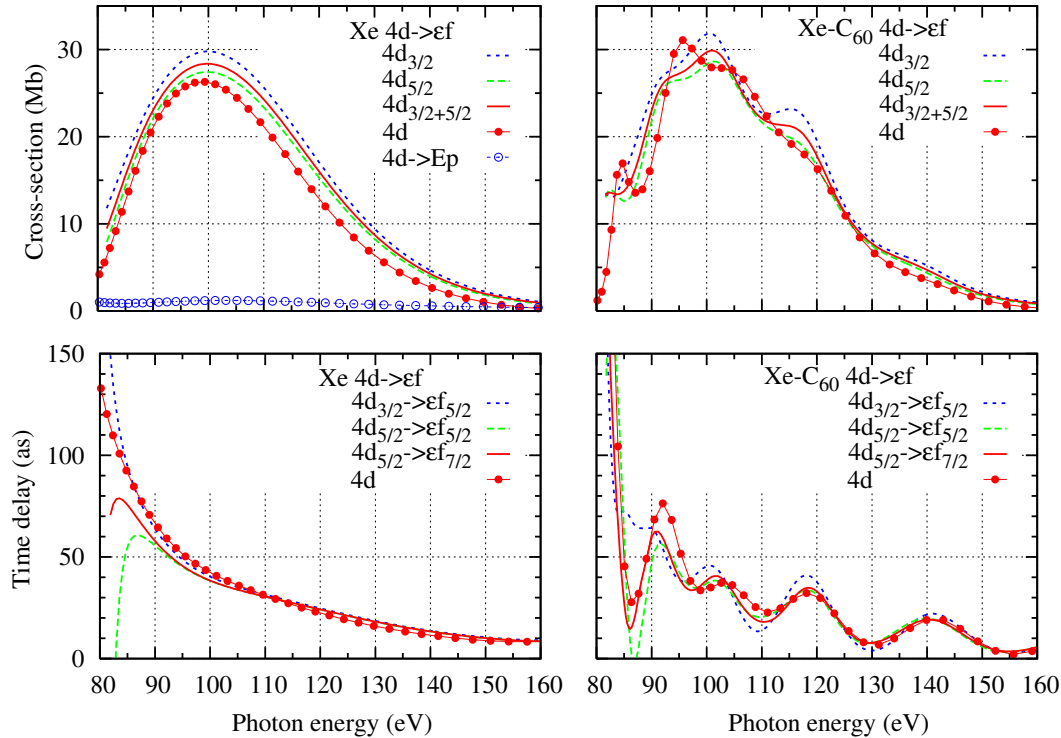

FIG. 2: Top: Partial photoionization cross-sections of the $4d$ shell in Xe (left) and Xe@C$_{60}$ (right). The RRPA calculations for spin-orbit resolved components $4d_{3/2}$ ($\times 5/2$), $4d_{5/2}$ ($\times 5/3$) and their sum are drawn with lines. The RPA calculations for the $4d \rightarrow \epsilon f$ and $4d \rightarrow \epsilon p$ (left panel only) cross-sections are drawn with line-dots. Bottom: time delay in photoionization of the $4d \rightarrow Ef$ channel of Xe (left) and Xe@C$_{60}$ (right). The RRPA calculations for various spin-orbit resolved components are drawn with lines while the RPA calculation is drawn with line-dots .

In conclusion, we have demonstrated clear presence of confinement resonances in photoelectron group delay (Wigner time delay) of the $4d$ shell of endohedrally confined Xe atom. These resonances have been observed recently in the $4d$ photoionization cross-section of Xe@C$_{60}$ [20]. Our calculations show that these resonances are even more prominent in the time delay. This result can stimulate further experimental studies by combination of an ionizing XUV pulse and a strobing IR pulse [3, 4]. In the present work we did not consider the influence of the IR field on the measured time delay. This effect, however, was analyzed in [23] where it was found that the laser

Coulomb coupling correction and the screening effect of the C$_{60}$ shell nearly totally cancel each other and hence the measured time delay will be essentially the Wigner time delay.

[1] A. Baltuška *et al*, *Attosecond control of electronic processes by intense light fields*, Nature **421**, 611 (2003).

[2] P. Eckle *et al*, *Attosecond ionization and tunneling delay time measurements in helium*, Science **322**(5907), 1525 (2008).

[3] M. Schultze *et al*, *Delay in Photoemission*, Science **328**(5986), 1658 (2010).

[4] K. Klünder *et al*, *Probing single-photon ionization on the attosecond time scale*, Phys. Rev. Lett. **106**(14), 143002 (2011).

[5] D. Guénot, K. Klünder, C. L. Arnold, D. Kroon, J. M. Dahlström, M. Miranda, T. Fordell, M. Gisselbrecht, P. Johnsson, J. Mauritsson, et al., *Photoemission-time-delay measurements and calculations close to the 3s-ionization-cross-section minimum in ar*, Phys. Rev. A **85**, 053424 (2012).

[6] V. S. Yakovlev, J. Gagnon, N. Karpowicz, and F. Krausz, *Attosecond streaking enables the measurement of quantum phase*, Phys. Rev. Lett. **105**(7), 073001 (2010).

[7] A. S. Kheifets and I. A. Ivanov, *Delay in atomic photoionization*, Phys. Rev. Lett. **105**(23), 233002 (2010).

[8] M. Ivanov and O. Smirnova, *How accurate is the attosecond streak camera?*, Phys. Rev. Lett. **107**, 213605 (2011).

[9] R. Pazourek, J. Feist, S. Nagele, and J. Burgdörfer, *Attosecond streaking of correlated two-electron transitions in helium*, Phys. Rev. Lett. **108**, 163001 (2012).

[10] C. A. A. de Carvalho and H. M. Nussenzveig, *Time delay*, Phys. Rep. **364**(2), 83 (2002).

[11] N. A. Cherepkov and S. K. Semenov, *On a complete experiment on photoionization of atoms*, J. Phys. B **37**(6), 1267 (2004).

[12] E. P. Wigner, *Lower limit for the energy derivative of the scattering phase shift*, Phys. Rev. **98**(1), 145 (1955).

[13] R. G. Newton, *Scattering Theory of Waves and Particles* (Courier Dover Publications, 1982).

[14] M. Saunders, H. A. Jiménez-Vázquez, R. J. Cross, and R. J. Poreda, *Stable compounds of helium and neon: He@C_{60} and Ne@C_{60}*, Science **259**(5100), 1428 (1993).

[15] M. J. Puska and R. M. Nieminen, *Photoabsorption of atoms inside C_{60}*, Phys. Rev. A **47**, 1181 (1993).

[16] M. Y. Amusia, A. S. Baltenkov, L. V. Chernysheva, Z. Felfli, and A. Z. Msezane, *Dramatic distortion of the 4d giant resonance by the C_{60} fullerene shell*, J. Phys. B **38**(10), L169 (2005).

[17] V. K. Dolmatov and S. T. Manson, *Correlation confinement resonances in photoionization of endohedral atoms: Xe@C_{60}*, J. Phys. B **41**(16), 165001 (2008).

[18] V. K. Dolmatov, in *Advances in Quantum Chemistry: Theory of Quantum Confined Systems*, edited by J. R. Sabin and E. Brandas (Academic Press, New York, 2009).

[19] M. E. Madjet, T. Renger, D. E. Hopper, M. A. McCune, H. S. Chakraborty, J.-M. Rost, and S. T. Manson, *Photoionization of Xe inside C_{60}: Atom-fullerene hybridization, giant cross-section enhancement, and correlation confinement resonances*, Phys. Rev. A **81**, 013202 (2010).

[20] A. L. D. Kilcoyne, A. Aguilar, A. Müller, S. Schippers, C. Cisneros, G. Alna'Washi, N. B. Aryal, K. K. Baral, D. A. Esteves, C. M. Thomas, et al., *Confinement resonances in photoionization of Xe@C_{60}^+*, Phys. Rev. Lett. **105**, 213001 (2010).

[21] J. Luberek and G. Wendin, *The Ba 4d-f giant dipole resonance as a probe of the structure of endohedral Ba@C_n metallofullerenes*, Chem. Phys. Lett. **248**(34), 147 (1996).

[22] G. Dixit, H. S. Chakraborty, and M. Madjet, *Time delay in the recoiling valence photoemission of Ar endohedrally confined in C_{60}*, Phys. Rev. Lett. **111**, 203003 (2013).

[23] S. Nagele, R. Pazourek, M. Wais, G. Wachter, and J. Burgdörfer, *Time-resolved photoemission using attosecond streaking*, J. Phys. Conf. Ser. p. arXiv 1401.6328 (2014).

[24] V. K. Dolmatov, J. L. King, and J. C. Oglesby, *Diffuse versus square-well confining potentials in modelling A@C_{60} atoms*, J. Phys. B **45**(10), 105102 (2012).

[25] N. A. C. M. Ya. Amus'ya and L. V. Chernysheva, *Cross section for the photoionization of noble-gas atoms with allowance for multielectron correlations*, Sov. Phys. – JETP **33**(1), 90 (1971).

[26] W. R. Johnson and C. D. Lin, *Multichannel relativistic random-phase approximation for the photoionization of atoms*, Phys. Rev. A **20**, 964 (1979).

[27] L. V. Chernysheva, N. A. Cherepkov, and V. Radojevic, *Self-consistent field Hartree-Fock program for atoms*, Comp. Phys. Comm. **11**, 57 (1976).

[28] L. V. Chernysheva, N. A. Cherepkov, and V. Radojevic, *Frozen core hartree-fock programm for atomic discrete and continuous states*, Comp. Phys. Comm. **18**, 87 (1979).

[29] S. S. Kumar, T. Banerjee, P. C. Deshmukh, and S. T. Manson, *Spin-orbit-interaction activated interchannel coupling in dipole and quadrupole photoionization*, Phys. Rev. A **79**, 043401 (2009).